

Strange Attractors of Memristor and Devil's Staircase to Chaos

Sadataka Furui

Graduate School of Teikyo University

2-17-12 Toyosatodai, Utsunomiya, 320-0003 Japan *

Tomoyuki Takano

IIX inc, Location 7F Daiichi Life Ins. Bld. Annex,

2-7-12 Nishi-Gotanda, Shinagawa-ku, Tokyo 141-0031, Japan †

July 17, 2018

Abstract

We made a chaotic memristic circuit proposed by Chua and analyzed the behavior of the voltage of the capacitor, electric current in the inductor and the voltage of the memristor by adding an external sinusoidal oscillation of a type $\gamma\omega \cos \omega t$ to $\dot{y}(t) \simeq \dot{i}_L(t)$, when the $\dot{x}(t) \simeq \dot{v}_C(t)$ is expressed by $y(t)/C$, and studied Devil's staircase route to chaos.

We compared the frequency of the driving oscillation f_s and the frequency of the response f_d in the window and assigned $W = f_s/f_d$ to each window. When capacitor $C = 1$, we observe stable attractors of Farey sequences $W = \{\frac{1}{2}, \frac{2}{3}, \frac{3}{4}, \frac{4}{5}, \dots, \frac{14}{15}, \frac{1}{1}\}$, which can be interpreted as hidden attractors, while when $C = 1.2$, we observe unstable attractors.

Possible role of octonions in the sequence is discussed.

**E-mail address:* furui@umb.teikyo-u.ac.jp

†*E-mail address:* takano_t@iix.co.jp

1 Introduction

In 1993, Hayes, Grebogi and Ott[1] discussed an electronic circuit in a chaotic regime, using the characterization of chaos as deterministic noise[2]. Typical evolution equation of the physical system is characterized by

$$\dot{\mathbf{x}}(t) = \mathbf{F}_\mu(\mathbf{x}(t)) \quad (1)$$

where \mathbf{x} is a set of coordinates in R^m and $F_\mu(\mathbf{x})$ determines the nonlinear time evolution. The nature of asymptotic motion depends upon the parameter μ and points where the change of asymptotic regime happens are called bifurcation points. The asymptotic motion follows an attractor in phase space, but its structure is not well understood, and unexpected stable attractors or chaotic attractors are observed. Chaos is characterized by sensitivity to the initial condition, or the dependence on the difference of orbits

$$d(t) = |\mathbf{s}'(t) - \mathbf{s}(t)| \sim e^{\lambda_1 t}. \quad (2)$$

The parameter λ_1 is called the largest Lyapunov coefficient.

How to measure the strangeness and the dimension of attractors was discussed by Grassberger and Procaccia[3]. In 1984, Grebogi et al.[4] showed that there are strange attractors whose Lyapunov exponents are negative. They showed that some chaotic attractors become nonstrange by certain weak perturbations, and the structure of Strange Nonchaotic Attractor (SNA) is rather complicated.

When a compact set S is covered by $N(r)$ cubes of edge length r , and each cube i is associated with the probability $p_i(r)$, we define the capacity dimension D_0 as

$$D_0 = \lim_{r \rightarrow 0} \frac{N(r)}{|\log r|},$$

and the information dimension D_1 as

$$D_1 = \lim_{r \rightarrow 0} \frac{H(r)}{\log r}$$

where

$$H(r) = \sum_{i=1}^{N(r)} p_i(r) \log p_i(r)$$

In [5], a differential equation of a pendulum

$$\begin{aligned} \frac{d^2\phi(t)}{dt^2} + \nu \frac{d\phi(t)}{dt} + g \sin \phi(t) \\ = F + G \sin(\omega_1 t + \alpha_1) + H \sin(\omega_2 t + \alpha_2), \end{aligned} \quad (3)$$

was studied, where ω_1 and ω_2 are incommensurate. They defined $\omega = \omega_1/\omega_2$ and considered a discrete map

$$\phi_{n+1} = F(\phi_n, \theta_n) \quad (4)$$

$$\theta_{n+1} = [\theta_n + 2\pi\omega] \quad (5)$$

where a square bracket indicates modulo 2π . They conjectured that $D_0 = 2$ and $D_1 = 1$. The structure of the attractor of dynamical systems whose Lyapunov exponents are non positive and which is defined by the two variables (x, θ) was studied by [6, 7, 8] and [9].

The conjecture on D_0 and D_1 were confirmed in [10]. Parameters that distinguish fractal torus configurations and chaotic configurations are important.

In 1971, Chua proposed that in addition to resistor, inductor and conductor, there is an interesting non-linear circuit element which is called memristor, a combination of memory and resistor [11]. Chua and Kang represented the dynamical system, which is called memristive system, by

$$\begin{aligned} \dot{x} &= f(x, u, t) \\ y &= g(x, u, t)u \end{aligned} \quad (6)$$

where u and y denote the input and the output of the system, respectively, and x denotes the state of the system[12]. Muthuswamy and Chua[13] showed that one can produce a non linear memristor, and combined with inductor, capacitor and opeamp, presented chaotic behaviors. The chaotic behavior of memristic system was analyzed in [14, 15, 16] and [17].

Chaos in electronic circuits that consists of capacitors, inductors, resistors and opeamp was studied in 1986 in [18]. When an external current source is added to the Chua's circuit, a Farey sequence period adding law was observed in [20]. Analyses of driven Chua's circuit were done in [23, 24] and in [25]. We analyzed the chaotic behaviors of Chua's circuit by adding an external current in the system[28]. In this paper, we add an external oscillation of current to the memristic system, which we call Muthuswamy-Chua's circuit

(MC circuit) and study changes in the chaotic behaviors due to an addition of driving currents.

Electrons are described by spinors and in the spinor theory of Cartan[30], self-dual vector field $X_i(i = 1, 2, 3, 4)$ is produced from spinors as a Plücker coordinate. Spinors are described by quaternions \mathcal{H} and bispinors that consist of two quaternions with a new imaginary unit l composes an octonion,

$$\mathcal{O} = \mathcal{H} + l\mathcal{H}$$

which has the automorphism: G_2 group. There are 24 dimensional bases in the G_2 group, and it has the triality symmetry. We study the electro magnetic field of the memristor using the octonion bases[31, 33, 34].

The paper is organized as follows. In Sect.2, we present chaos in Chua's circuit, and in Sect.3 we present Chaos in Memristic circuit. In Sect.4, Strange nonchaotic attractor in driven memristor is studied, and in Sect.5, the resonance frequency of the driven MC circuit is analyzed by using octonion basis. Difference of strange chaotic attractors and strange nonchaotic attractor (SNA) are discussed in Sect.6.

2 Chaos in Chua's circuit

Chua's circuit consists of an autonomous circuit which contains a three-segments piecewise-linear resistor, two capacitors, one inductor and a variable resistor [18]. The equation of the circuit is described by the coupled differential equation

$$\begin{cases} C_1 \frac{d}{dt} v_{C1} = G(v_{C2} - v_{C1}) - \tilde{g}(v_{C1}, m_0, m_1) \\ C_2 \frac{d}{dt} v_{C2} = G(v_{C1} - v_{C2}) + i_L \\ L \frac{d}{dt} i_L = -v_{C2} \end{cases} \quad (7)$$

The three-segment piecewise-linear resistor which constitutes the non-linear element is characterized by

$$\tilde{g}(v_{C1}, m_0, m_1) = (m_1 - m_0)(|v_{C1} + B_p| - |v_{C1} - B_p|)/2 + m_0 v_{C1},$$

where B_p is chosen to be 1V, m_0 is the slope (mA/V) outside $|v_{C1}| > B_p$ and m_1 is the slope inside $-B_p < v_{C1} < B_p$.

Here v_{C1} and v_{C2} are the voltages of the two capacitors (in V), i_L is the current that flows in the inductor (in A), C_1 and C_2 are capacitance (in F),

L is inductance (in H), and G is the conductance of the variable resistor (in Ω^{-1}).

The function $\tilde{g}(v_{C1}, m_0, m_1)$ can be regarded as an active resistor. If it is locally passive, the circuit is tame, but when it is locally active, it keeps supplying power to the external circuit. The chaotic behavior is expected to be due to the power dissipated in the passive element. A difference from the van der Pol circuit is that the passive area and the active area are not separated by the strange attractor, but they are entangled. The orbit in the $v_{C1} - v_{C2}$ plane shows a double scroll orbit or a hetero-clinic orbit (i.e. an orbit which starts from a fixed point to another fixed point). We assign v_{C1}, v_{C2} and i_L , with a specific normalization, x, y and z , respectively.

We did not control chaotic circuits by triggering simple electronic pulse as [19], when the orbit arrives in a certain region which we assigned 'e' in Fig.8 of [28] from which complication of the orbit starts. Main difference from [19] was that we have chosen a proper height of the pulse, so that the periodic trajectory was kept and we did not need to reset the current.

$$\begin{cases} \dot{x} = \alpha(y - h(x)) \\ \dot{y} = x - y + z \\ \dot{z} = -\beta y \end{cases} \quad (8)$$

where

$$h(x) = m_1 x + \frac{1}{2}(m_0 - m_1)[|x + 1| - |x - 1|]$$

$$h(x) = \begin{cases} m_1 x + (m_0 - m_1) & x \geq 1 \\ m_0 x & |x| \leq 1 \\ m_1 x - (m_0 - m_1) & x \leq -1 \end{cases}$$

is a piecewise linear equation.

We observed that periodic double scroll is running on heteroclinic orbits. A periodic double scroll can be moved to a homoclinic orbit (i.e. an orbit which has single fixed point) by triggering a pulse when the orbit arrives at a certain region. A simulation of the Chua's circuit was done in [23]. Sinusoidally driven Chua's circuit was shown to have the Arnold's tongue and devil's staircase structure in the dynamical structure of the voltage[20], and the sinusoidally-driven double scroll Chua circuit was analyzed by Baptista and Caldas[24].

Bifurcation and routes to chaos in other sinusoidally-driven extended Chua circuits was discussed by Thamilmaran and Lakshmanan[25]. In 2010,

Leonov, Vagaitsev and Kuznetsov[26] claimed that there appear hidden attractors in a n dimensional system with continuous vector function $\Psi(x)$ ($\Psi(0) = 0$) and a constant $n \times n$ matrix P ,

$$\frac{d\mathbf{x}}{dt} = P\mathbf{x} + \Psi(\mathbf{x}).$$

To find a periodic solution close to the harmonic oscillation, they considered a matrix K , such that $P_0 = P + K$ has a pair of purely imaginary eigenvalues $\pm i\omega_0$ ($\omega_0 > 0$) and other eigenvalues of P_0 have negative real parts. They introduced a finite sequence of continuous functions $\phi^0(\mathbf{x}), \phi^1(\mathbf{x}), \dots, \phi^m(\mathbf{x})$, such that $\phi^0(\mathbf{x})$ is small and $\phi^m(\mathbf{x}) = \phi(\mathbf{x})$. They took sufficiently long period $[0, T]$ and considered

$$\frac{d\mathbf{x}}{dt} = P_0\mathbf{x} + \phi^0(\mathbf{x}), \quad \frac{d\mathbf{x}}{dt} = P_0\mathbf{x} + \phi^j(\mathbf{x}), \quad (j = 1, \dots, m)$$

with initial condition $\mathbf{x}^j(0) = \mathbf{x}^{j-1}(T)$. They showed that chaotic attractors can be produced by the perturbation. The review of chaotic hidden attractors in Chua's circuit is given in[27].

3 Chaos in Muthuswamy-Chua's circuits

In the study of chaotic behaviors in electronic circuits, Chua's electronic devices have attracted constant research interests.

In 2010, Muthuswamy and Chua[13] showed that a system with an inductor, capacitor and non-linear memristor can produce a chaotic circuit. The three-element circuit with the voltage across the capacitor $x(t) = v_C(t)$, the current through the inductor $y(t) = i_L(t)$ and the internal state of the memristor $z(t)$ satisfy the equation

$$\begin{cases} \dot{x} = \frac{y}{C} \\ \dot{y} = \frac{1}{L}[x + \beta(z^2 - 1)y] \\ \dot{z} = -y - \alpha z + yz. \end{cases} \quad (9)$$

We produced the similar circuit element as MC, measured the current through the inductor, and the voltage across the capacitor. We choose

$$C = I_s C_n T_s$$

$$\begin{aligned}
L &= \frac{L_n T_s}{I_s} \\
\beta &= \frac{\beta_{5kpot}}{R} \\
\alpha &= \frac{1}{T_s C_f \alpha_{10kpot}}
\end{aligned} \tag{10}$$

where $I_s = 10000$, $C_n = 1\text{nF}$, $T_s = 10^5$, $L_n = 360\text{mH}$, $R = 1\text{k}\Omega$, $C_f = 10\text{nF}$.

The chaotic attractor $i_L(t) = y$ versus $v_C(t) = x$ obtained by experiment is shown in Fig.1. Here we took $\beta = 1.43$

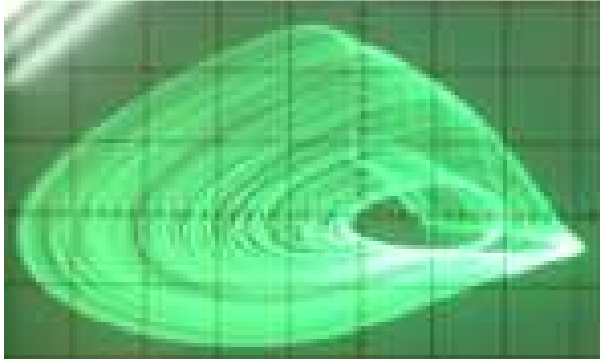


Figure 1: The chaotic attractor $i_L(t)$ versus $v_C(t)$. Experimental result.

When $\dot{z} = 0$, the eq. (9) becomes $-\alpha z + (z - 1)y = 0$ and $z = \frac{y}{y - \alpha}$.

MC defined memristor equation by replacing y by i_M and $v_L + v_c = v_M$ as

$$\begin{aligned}
v_M(t) &= \beta(z^2 - 1)i_M(t) \\
\dot{z} &= i_M(t) - \alpha z - i_M(t)z
\end{aligned} \tag{11}$$

and by choosing $\dot{z} = 0$, the DC characteristic becomes

$$v_M(t) = \beta \left(\frac{i_M(t)^2}{(i_M(t) + \alpha)^2} - 1 \right) i_M(t) \tag{12}$$

When $C=1$, $L=3.3$ and $\alpha = 0.2$, and the DC characteristic is chosen, solution of the eq.(12) which yields Lorentz like attractor becomes Fig.2, and the DC $v_M - i_M$ plot becomes Fig.3.

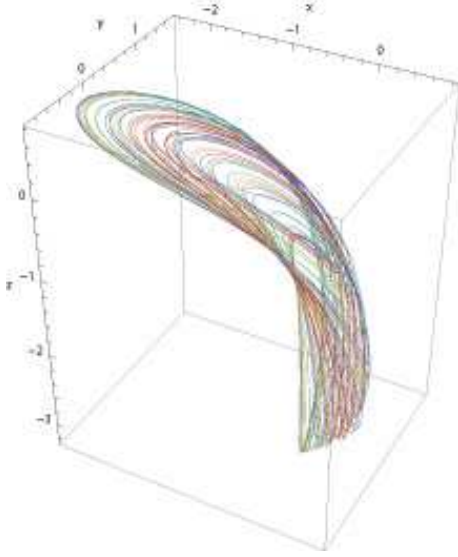


Figure 2: The attractor in the xyz-space of $C=1, L=3.3, \alpha = 0.2, \beta = 0.5$. Numerical simulation.

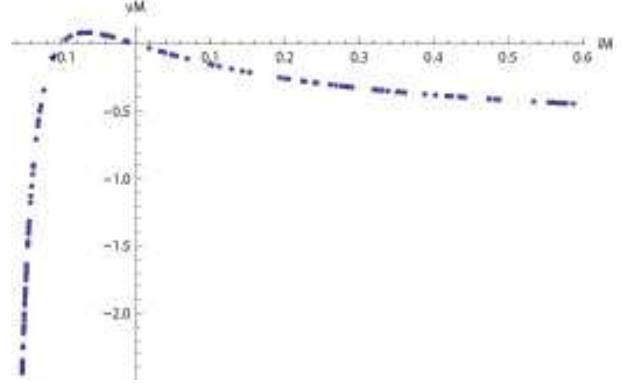


Figure 3: The DC $v_M - i_M$ plot at $C = 1, L = 3.3, \alpha = 0.2$.

The bifurcation diagram and the Lyapunov exponent λ for $C = 1, L = 3.3$ and $\alpha = 0.2$ as a function of β are shown in Fig.3. The diagram shows that a bifurcation occurs at $\beta = 1.23, 1.52$ and 1.58 and two circuits, four circuits and eight circuits, respectively appear.

The Fig.4 shows that in the region $1.5 < \beta < 1.8$ the Lyapunov exponent λ is positive and about 0.04 , and the bifurcation diagram is chaotic.

Ginoux, Letelier and Chua[16] calculated the flow curvature manifold of the memristor. Our result is consistent with their results.

4 Strange nonchaotic attractor in driven Muthuswamy-Chua's circuit

We added external input voltage $F = \gamma \sin \omega t$ and considered the system of the equation

$$\begin{cases} \dot{x} = \frac{y}{C} \\ \dot{y} = \frac{-1}{L}[x + \beta(z^2 - 1)y + \gamma \sin \omega t] \\ \dot{z} = -y - \alpha z + yz \end{cases} \quad (13)$$

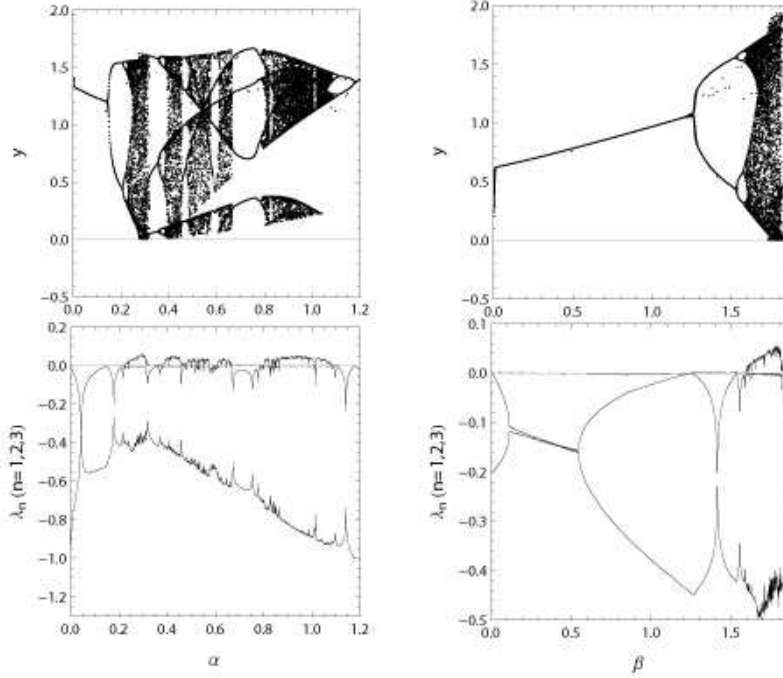


Figure 4: The bifurcation diagram and the Lyapunov exponent of Memristor. $C=1, L=3.3$

Strange nonchaotic attractor in periodically driven systems were investigated in [29] and it was argued that without external oscillation, i.e. in autonomous systems it is difficult to find a SNA, but in periodically driven systems, SNAs had been observed. We want to investigate details of chaos and SNAs in driven MC circuits. When $\gamma = 0.01$ i.e. very small, dependence of y as a function of ω is chaotic. However, when we fixed $C = 1.2$ and $\gamma = 0.2$, and modified ω from 0.01 to $\omega = 1$ we found a wide window of period 1 at around $\omega = 0.51$, as shown in Fig.7.

In the region $0.51 \leq \omega \leq 0.62$ the period of the external voltage agrees with the eigenperiod of the system

$$\frac{1}{LC}T_s = \frac{1}{\sqrt{3.3}}T_s = 0.55T_s. \quad (14)$$

The corresponding frequency is $f\omega T_s = 7.3\text{kHz}$ (8.8kHz in the case of $C = 1$).

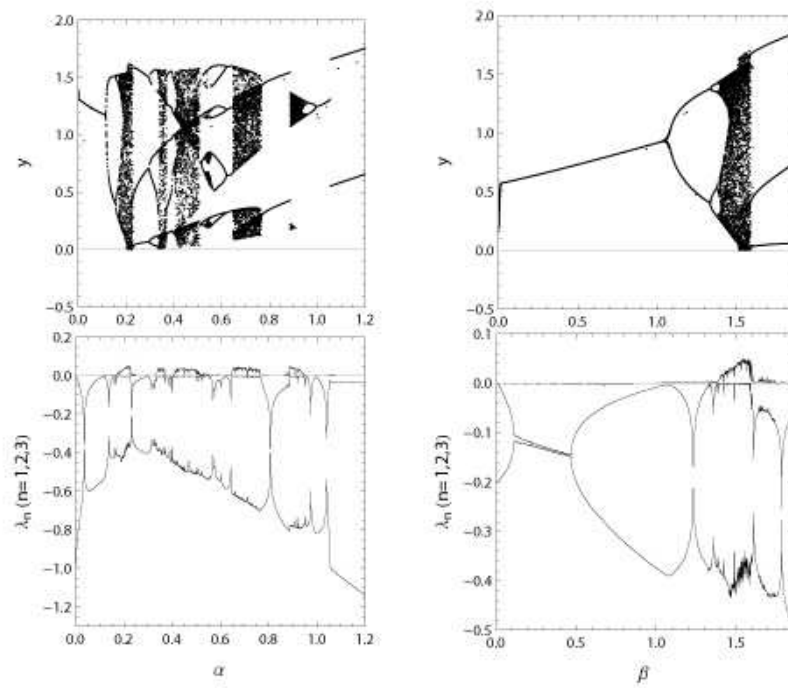


Figure 5: The bifurcation diagram and the Lyapunov exponent of Memristor. $C = 1.2, L = 3.3$.

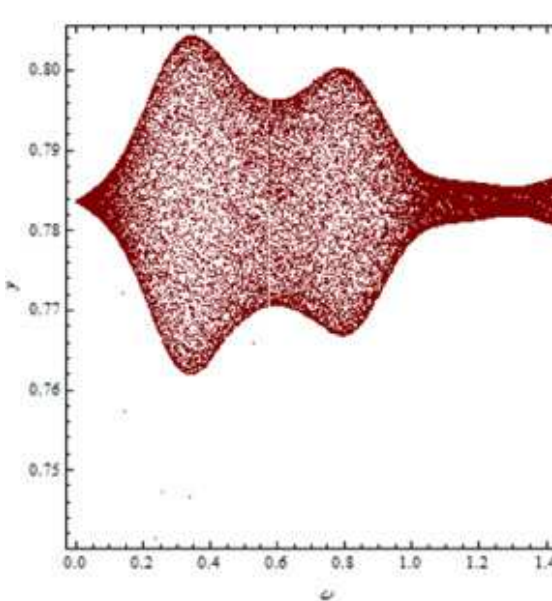


Figure 6: The bifurcation diagram $C = 1, L = 3.3, \alpha = 0.2, \beta = 0.5, \gamma = 0.01$.

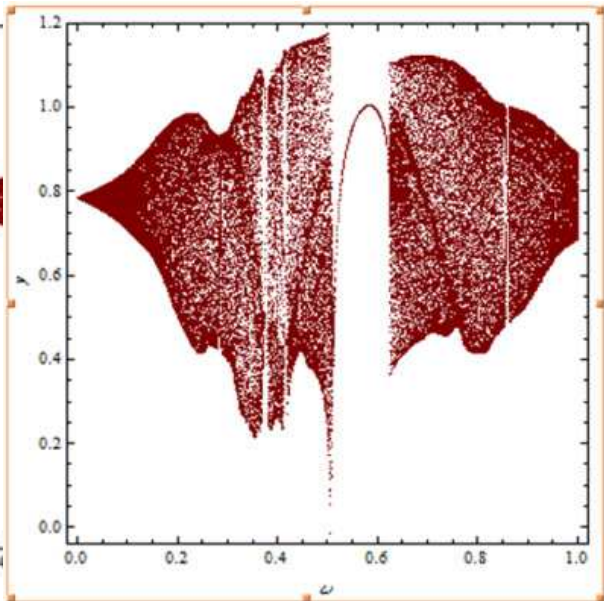


Figure 7: The bifurcation diagram $C = 1, L = 3.3, \alpha = 0.2, \beta = 0.5, \gamma = 0.2$.

In Fig.6, we present the bifurcation diagram of the system with $C = 1, L = 3.3, \alpha = 0.2, \beta = 0.5, \gamma = 0.2$. We find nonchaotic strange attractor in this case.

The bifurcation diagrams of the system with $C = 1.2, L = 3.3, \alpha = 0.2, \beta = 0.5, \gamma = 0.2$, in the range $0.24 \leq \omega \leq 0.36$ and $0.36 \leq \omega \leq 0.46$ are shown in Fig.8 and in Fig.9, respectively, together with the frequency of the response f_d .

We present the Lyapunov exponent λ in Fig.10. When $\omega \sim 0.3605$, λ becomes slightly positive up to about 0.01. The Lyapunov exponents are negative in other windows.

The frequency of the windows ω as a function of the number of nodes of the response for samples of $C = 1$ is shown in Fig.11. In the case of one node, we put the ω at $f_d = 8$, since when we put ω/f_d as a function of the number of node f_d , the ω of one node divided by 8 becomes close to that of node 7. The ω/n for samples of $C = 1.2$ are shown in Fig.12. It contains the series from $f_d = 2$ to 9, from 9 to 17, from 5 to 7 and from 8 to 11, which are shown by different colors. The single period window may be considered as

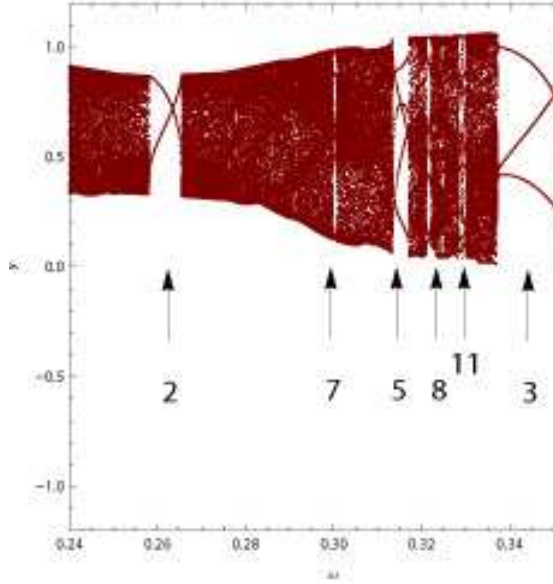


Figure 8: The bifurcation diagram of the driven memristor. $C = 1.2, L = 3.3, 0.24 \leq \omega \leq 0.36$.

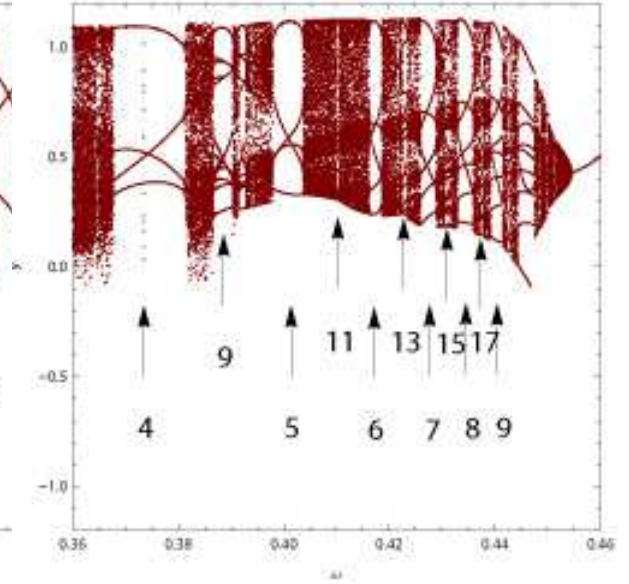


Figure 9: The bifurcation diagram of the driven memristor. $C = 1.2, L = 3.3, 0.36 \leq \omega \leq 0.46$.

8 degenerate nodes. The energy $\omega/8$ of this node put at $n = 8$ is consistent with ω/f_d of $f_d = 7$, i.e. energy per node of $f_d = \text{Mod}(-1, 8) = 7$.

The matching ω/f_d in the case of $C = 1$ is about 10% lower than that of $C = 1.2$, and the width of the window of $C = 1$ is narrower than that of $C = 1.2$.

The attractor of $n = 1$ of samples $C = 1.2, L = 3.3$ at $\omega = 0.51$ is shown in Fig.13, and the time series of $x(t), y(t), z(t)$ are compared with $\gamma \sin \omega t$ in Fig.14. Since the frequency of the response and that of driving term are both equal to 1, the ratio of $W = f_s/f_d = 1/1$

At windows of nodes of $f_d = 2$ to $f_d = 9$ of samples $C = 1.2, L = 3.3$, we compared the time series $x(t)$ of the response and input $\gamma \sin \omega t$. The observed ratio $W = f_s/f_d$ turned out to be

$$\left\{ \frac{1}{2}, \frac{2}{3}, \frac{3}{4}, \frac{4}{5}, \frac{5}{6}, \frac{6}{7}, \frac{7}{8}, \frac{8}{9}, \frac{1}{1} \right\}.$$

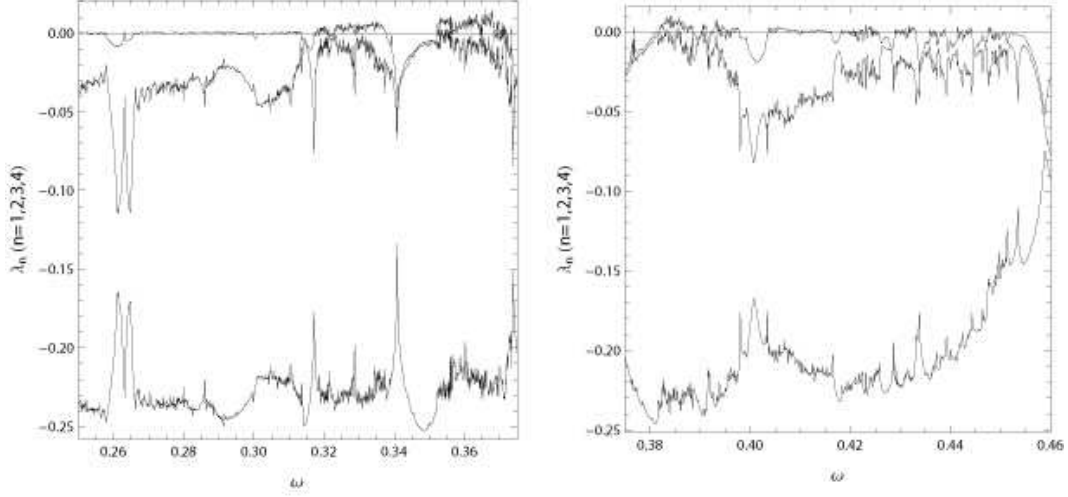


Figure 10: The Lyapunov exponent of Memristor. $C = 1.2, L = 3.3, \alpha = 0.2, \beta = 0.5, \gamma = 0.2$.

The sequence follows the period adding law[20]

$$\frac{q}{p} \rightarrow \frac{q+Q}{p+P} \rightarrow \frac{q+2Q}{p+2P} \rightarrow \dots \rightarrow \text{chaos} \rightarrow \frac{Q}{P}$$

The time series $x(t)$ and $\gamma \sin \omega t$ at $\omega = 0.4$ allows an assignment of $W = 4/5$.

Between the window of $f_d = 2$ and $f_d = 3$, we found a window of $f_d = 5 = 2 + 3$, which appears from the Farey sum

$$\frac{1}{2} + \frac{2}{3} \rightarrow \frac{3}{5}$$

A comparison of the time series $x(t)$ and the corresponding $\gamma \sin \omega t$ at $\omega = 0.315$ allows the assignment $W = 3/5$. This new node of $W = 3/5$ and the node of $W = 1/2$ make a node of $f_d = 7 = 5 + 2$. A comparison of the time series $x(t)$ and the corresponding $\gamma \sin \omega t$ at $\omega = 0.300$ allows the assignment $W = 4/7$ as shown in Fig.15. The new W again appears from the Farey sum

$$\frac{1}{2} + \frac{3}{5} \rightarrow \frac{4}{7}$$

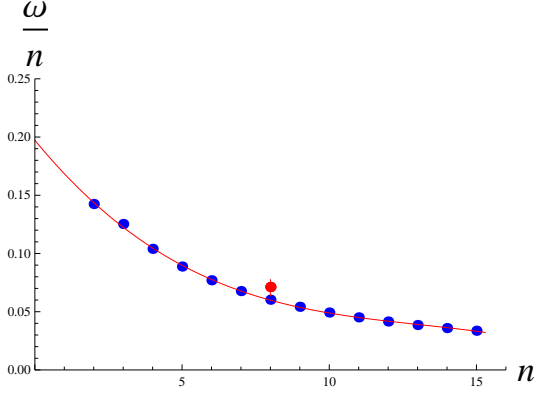


Figure 11: The fit of ω/n as a function of torus loop n . $C = 1$

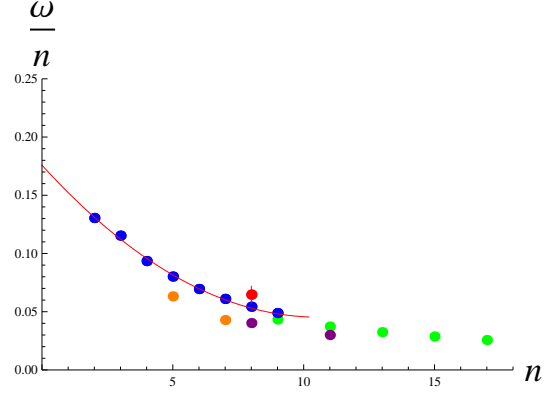


Figure 12: The fit of ω/n as a function of torus loop n . $C = 1.2$

The time series of $x(t)$ and $\gamma \sin \omega t$ of $W = 6/7$ are shown in Fig.16 for comparison.

A similar comparison of $f_d = 8$ data, $W = \frac{2}{3} + \frac{3}{5} \rightarrow \frac{5}{8}$ and $W = \frac{7}{8}$ are shown in Fig.17 and Fig.18, respectively.

We compared, also $f_d = 9$ data, $W = \frac{3}{4} + \frac{4}{5} \rightarrow \frac{7}{9}$ and $W = \frac{8}{9}$.

The series

$$\left\{ \frac{3}{5}, \frac{4}{7}, \dots, \frac{1}{2} \right\}$$

follows the period adding law[20] with $q = 3, Q = 1, p = 5, P = 2$. The series

$$\left\{ \frac{5}{8}, \frac{7}{9}, \dots, \frac{2}{1} \right\}$$

follows the period adding law with $q = 5, Q = 2, p = 8, P = 1$.

There are other Farey sums

$$\frac{4}{5} + \frac{5}{6} \rightarrow \frac{9}{11}, \quad \text{upto} \quad \frac{7}{8} + \frac{8}{9} \rightarrow \frac{15}{17}$$

from $\omega = 0.41$ until $\omega = 0.4375$, which make the series of W

$$\left\{ \frac{9}{11}, \frac{11}{13}, \frac{13}{15}, \frac{15}{17}, \frac{2}{2} \right\}.$$

Near the region of $\omega = 0.45$, there is a window which has 10 nodes from left cluster and 9 nodes from right cluster as shown in Fig.9. We assign

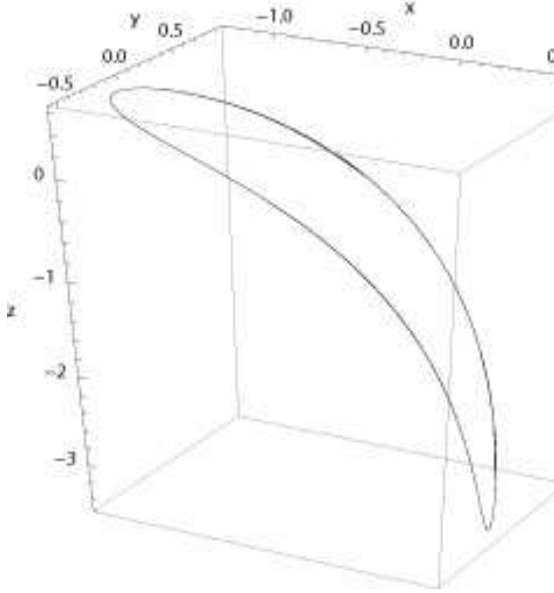


Figure 13: The attractor of $f_d = 1$. $C = 1.2, L = 3.3, \alpha = 0.2, \beta = 0.5, \gamma = 0.2$

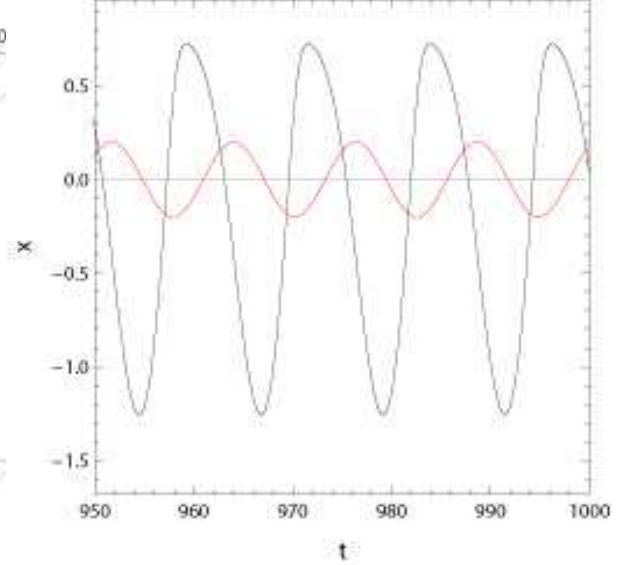


Figure 14: The time series of $x(t)$ and $\gamma \sin \omega t$. $\omega = 0.51, W = 1/1, C = 1.2, L = 3.3$

$W = \left\{ \frac{9}{9}, \frac{8}{8}, \frac{7}{7} \right\}$ at $\omega = 0.446, 0.450$ and 0.4515 , respectively, and the Farey sums

$$\frac{8}{9} + \frac{9}{9} \rightarrow \frac{17}{18}, \quad \text{and} \quad \frac{9}{9} + \frac{8}{8} \rightarrow \frac{17}{17}$$

at $\omega = 0.4425$ and $\omega = 0.448$, respectively.

The bifurcation diagram shows that when $\omega = 0.3605$, the system is chaotic. We studied Poincaré map of driven MC circuit at this $\omega = 0.3605$ by taking the Poincaré map on the xy plane, yz plane and xz plane.

The points are plotted, when ωt satisfies $Mod[\omega t, 2\pi] = 0$. We calculated the Poincaré map of $\omega = 0.3605$ on xy, yz and xz plane, which are shown in Fig.19, 20 and 21.

In the case of oscillation on the xy plane, we calculated $\Theta_n = \tan^{-1}(y_n/x_n)$, where x_n and y_n are the x and y coordinates of the Poincaré map. The return map of Θ_{n+1} v.s. Θ_n simplifies the chaotic behaviors. It becomes a single line in the case of $\omega < 0.26$, four clusters when $\omega = 0.3$, and chaotic when $\omega = 0.32$. When $\omega = 0.5$, clusters appear again, and when $\omega = 0.6$, a single line appears again.

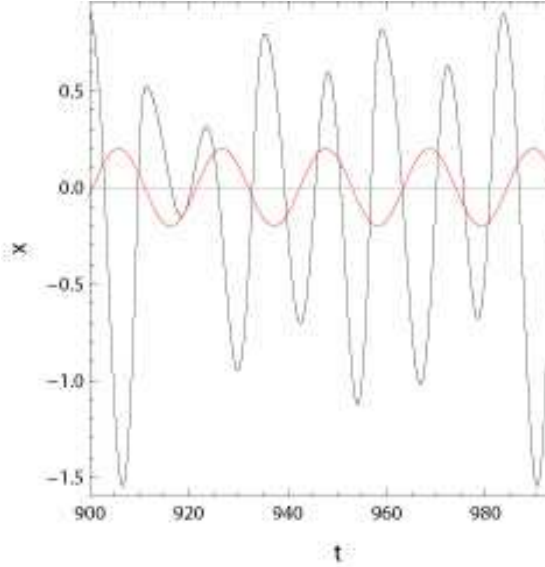


Figure 15: The time series of $x(t)$ and $\gamma \sin \omega t$. $\omega = 0.30, W = 4/7, C = 1.2, L = 3.3$

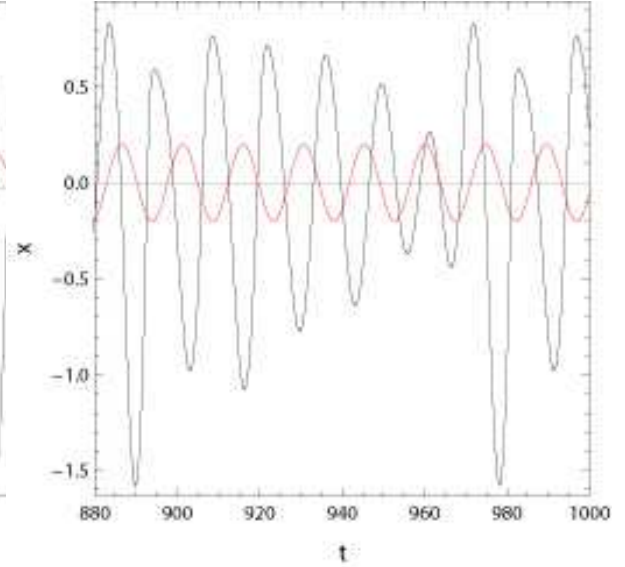


Figure 16: The time series of $x(t)$ and $\gamma \sin \omega t$. $\omega = 0.427, W = 6/7, C = 1.2, L = 3.3$

We observed that except near $\omega = 0.36$, λ is negative, and the oscillation is non-chaotic in most regions.

In the case of $C = 1.2$, we observed Windows= $\{\frac{1}{2}, \dots, \frac{8}{9}\}$, i.e. 8 levels were observed, (The level $\frac{9}{10}$ is broken in the high-frequency part.) and above the level $\frac{4}{5}$ the level $\frac{7}{9}$ in the Farey sequence $\{\frac{3}{4}, \frac{7}{9}, \frac{4}{5}\}$ is made and the sequence $\{\frac{9}{11}, \dots, \frac{15}{17}\}$ follows.

Below the level $\frac{7}{9}$ the Farey sequences are different, and as the source of 8 levels in the $C = 1.2$ case, we imagine a combination of the input electron and the output electron both expressed by quaternions. Two quaternions can make an octonion which couples with 8 dimensional vector fields.

In the case of $C = 1.0$ and $\gamma = 0.2$, ω of the node $W = \frac{1}{1}$ is about 10% larger than that of $C = 1.2$, and the node n at highest ω was assigned up to 15, in contrast to up to 8 in the case of $C = 1.2$.

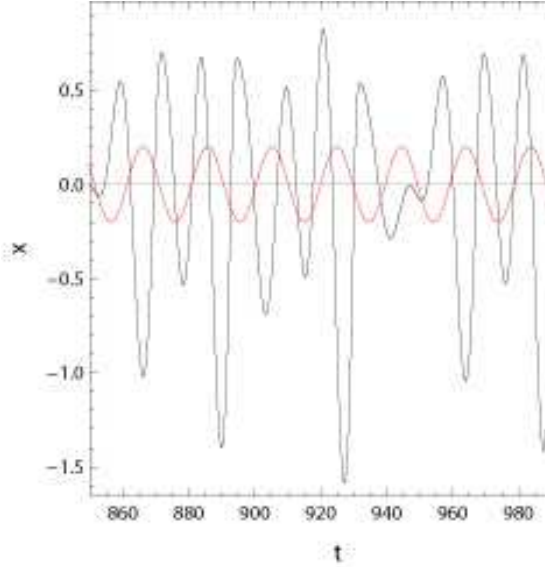


Figure 17: The time series of $x(t)$ and $\gamma \sin \omega t$. $\omega = 0.321, W = 5/8, C = 1.2, L = 3.3$

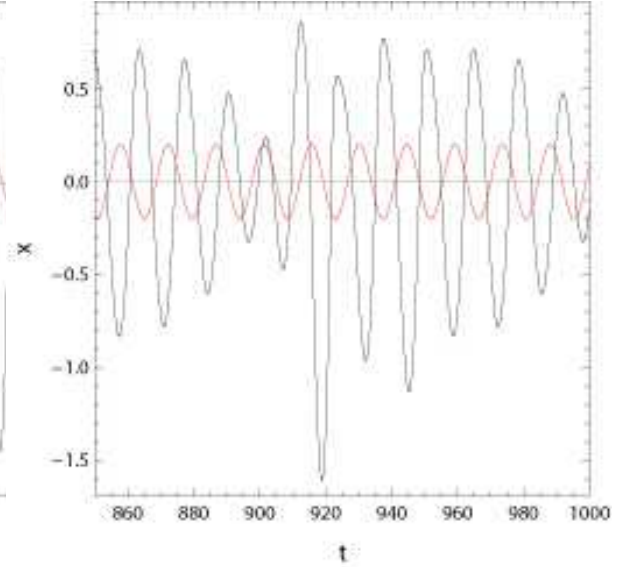


Figure 18: The time series of $x(t)$ and $\gamma \sin \omega t$. $\omega = 0.434, W = 7/8, C = 1.2, L = 3.3$

The width of the windows is narrower, and the sequences of W consist of

$$\left\{ \frac{1}{2}, \frac{2}{3}, \frac{3}{4}, \frac{4}{5}, \frac{5}{6}, \frac{6}{7}, \frac{7}{8}, \frac{8}{9}, \frac{9}{10}, \frac{10}{11}, \frac{11}{12}, \frac{12}{13}, \frac{13}{14}, \frac{14}{15}, \frac{1}{1} \right\}.$$

The Farey sequences of $P \neq Q$ like $W = \left\{ \frac{3}{5}, \frac{4}{7} \right\}$ and $W = \left\{ \frac{5}{8}, \frac{7}{9} \right\}$, which were observed in $C = 1.2$, were not observed in $C = 1.0$.

Extending this analysis to the lower frequency region, we observed the devil's staircase structure[32] in the case of $C = 1$ as Fig.22 and in the case of $C = 1.2$, as Fig.23.

The qualitative difference of the case of $C = 1$ and $C = 1.2$ can be explained by the hidden attractor[26, 27]. They showed that when there is a perturbation with amplitude small enough, the Poincaré map of F of the set Ω of solutions of the differential equation into itself

$$F\Omega \subset \Omega$$

can introduce stable solutions. When $C = 1.2$ the $F\Omega$ goes outside Ω and unstable solutions dominate, but when $C = 1$, there appear solutions of $f_s < f_d$ and hidden attractors appear.

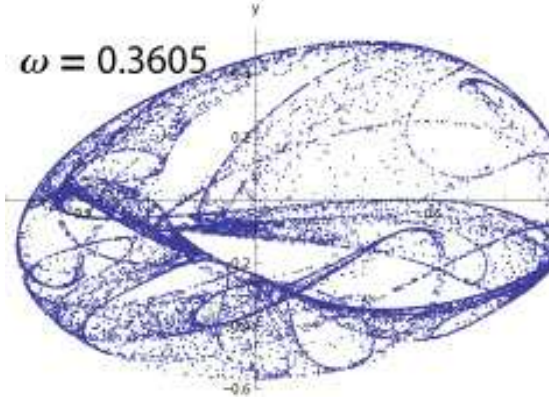


Figure 19: The Poincaré map on the xy plane. $\omega = 0.3605$.

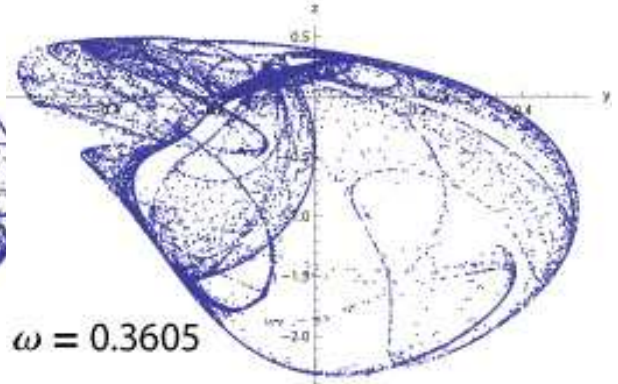


Figure 20: The Poincaré map on the yz plane. $\omega = 0.3605$.

5 Conjecture on the frequency of the windows of driven Muthuswamy-Chua's circuit

The four component Dirac's spinor is a combination of two two-component spinors each transforms as a quaternion. É. Cartan[30] defined, using semi-spinors of an even number of indices

$$\xi_{even} := \xi_{12}, \xi_{23}, \xi_{34}, \xi_{13}, \xi_{24}, \xi_{14}, \xi_{1234}, \xi_0$$

and semi-spinors of an odd number of indices

$$\xi_{odd} := \xi_1, \xi_2, \xi_3, \xi_4, \xi_{234}, \xi_{134}, \xi_{124}, \xi_{123},$$

for bases of spinors

In octonion basis, we consider a fermion ϕ and its charge conjugate $C\phi$ [31, 34], which are described by

$$\begin{aligned} \mathcal{A} &= \xi_0 I + \xi_{14} \sigma_x + \xi_{24} \sigma_y + \xi_{34} \sigma_z \\ &= \begin{pmatrix} A_4 + i A_3 & i A_1 - A_2 \\ i A_1 + A_2 & A_4 - i A_3 \end{pmatrix} \end{aligned}$$

$$\begin{aligned} \mathcal{B} &= \xi_{1234} I - \xi_{23} \sigma_x - \xi_{31} \sigma_y - \xi_{12} \sigma_z \\ &= \begin{pmatrix} B_4 - i B_3 & -i B_1 + B_2 \\ -i B_1 - B_2 & B_4 + i B_3 \end{pmatrix} \end{aligned}$$

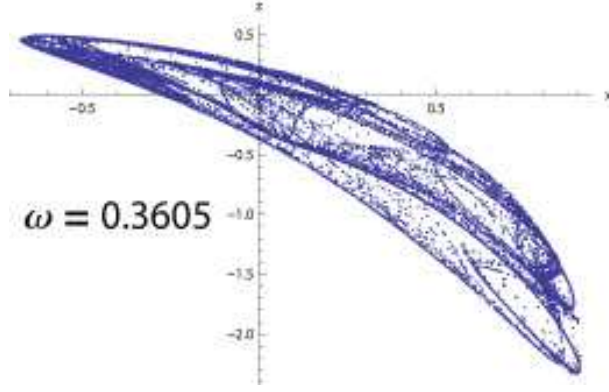


Figure 21: The Poincaré map on the xz plane. $\omega = 0.3605$.

and anti-fermion ψ and its charge conjugate $C\psi$, which are described by

$$\begin{aligned} \mathcal{C} &= \xi_4 I + \xi_1 \sigma_x + \xi_2 \sigma_y + \xi_3 \sigma_z \\ &= \begin{pmatrix} C_4 + i C_3 & i C_1 - C_2 \\ i C_1 + C_2 & C_4 - i C_3 \end{pmatrix} \end{aligned}$$

$$\begin{aligned} \mathcal{D} &= \xi_{123} I - \xi_{234} \sigma_x - \xi_{314} \sigma_y - \xi_{124} \sigma_z \\ &= \begin{pmatrix} D_4 - i D_3 & -i D_1 + D_2 \\ -i D_1 - D_2 & D_4 + i D_3 \end{pmatrix}. \end{aligned}$$

The coupling of the spinor and vectors defined by Cartan is,

$$\begin{aligned} \mathcal{F} &= {}^t \phi C X \psi \\ &= x^1 (-A_1 D_4 - B_2 D_3 + B_3 D_2 + B_4 C_1) \\ &\quad + x^2 (B_1 D_3 - A_2 D_4 - B_3 D_1 + B_4 C_2) \\ &\quad + x^3 (-B_1 D_2 + B_2 D_1 - A_3 D_4 + B_4 C_3) \\ &\quad + x^4 (-A_1 D_1 - A_2 D_2 - A_3 D_3 + B_4 C_4) \\ &\quad + x^{1'} (B_1 C_4 - A_2 C_3 - A_3 C_2 - A_4 D_1) \\ &\quad + x^{2'} (A_1 C_3 + B_2 C_4 - A_3 C_1 - A_4 D_2) \\ &\quad + x^{3'} (-A_1 C_2 + A_2 C_1 + B_3 C_4 - A_4 D_3) \\ &\quad + x^{4'} (-B_1 C_1 - B_2 C_2 - B_3 C_3 + A_4 D_4). \end{aligned}$$

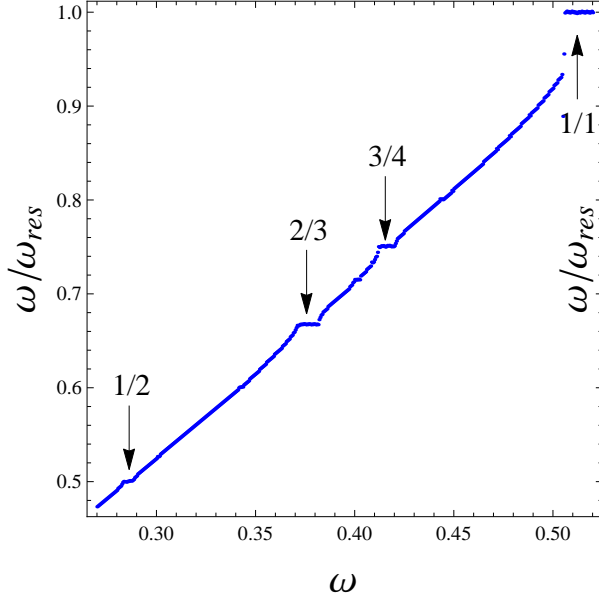


Figure 22: The devil's staircase for $C = 1$.

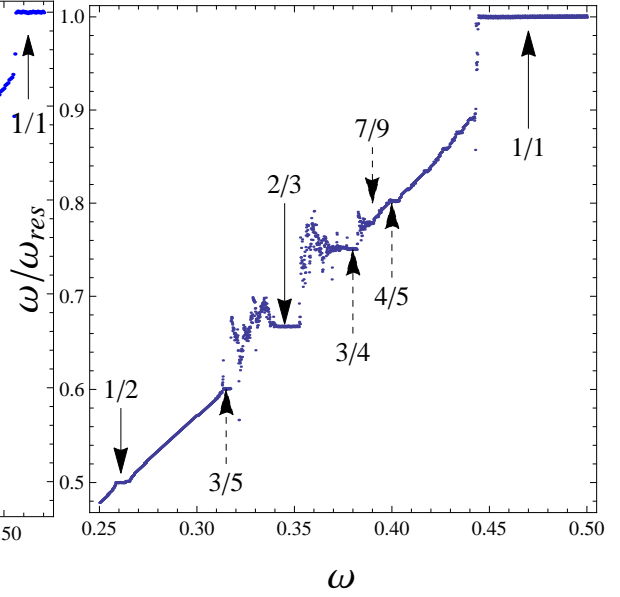


Figure 23: The devil's staircase for $C = 1.2$.

In our system, there are an input electron which is represented by the plane wave, and an output fermion. There are 4 possible choices of the input fermion wave functions $\mathcal{A}, \mathcal{B}, \mathcal{C}, \mathcal{D}$, and 2 possible types of exchanged photons i.e. left vertex and right vertex are the same x_4 or x'_4 exchange, and left vertex is x_4 and right vertex is x'_4 or vice versa, which we denote x_4/x'_4 exchange. Thus, there are 8 types of interactions.

The exchange of x_4 between a particle

$$\tilde{\mathcal{A}} = \begin{pmatrix} B_4 + i A_3 & i A_1 - A_2 \\ i A_1 + A_2 & B_4 - i A_3 \end{pmatrix} = (\vec{A}, B_4)$$

and another particle

$$\tilde{\mathcal{D}} = \begin{pmatrix} C_4 + i D_3 & i D_1 - D_2 \\ i D_1 + D_2 & C_4 - i D_3 \end{pmatrix} = (\vec{D}, C_4)$$

is represented in Fig.24.

The exchange of x'_4 between a hole

$$\tilde{\mathcal{B}} = \begin{pmatrix} A_4 + i B_3 & i B_1 - B_2 \\ i B_1 + B_2 & A_4 - i B_3 \end{pmatrix} = (\vec{B}, A_4)$$

and another hole

$$\tilde{\mathcal{C}} = \begin{pmatrix} D_4 + iC_3 & iC_1 - C_2 \\ iC_1 + C_2 & D_4 - iC_3 \end{pmatrix} = (\vec{\mathcal{C}}, D_4)$$

is represented in Fig.25.

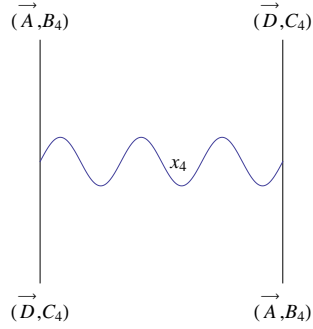


Figure 24: The vector x_4 exchange between a particle-particle $(\vec{D}, C_4), (\vec{A}, B_4)$.

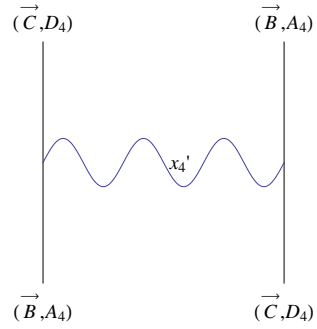


Figure 25: The vector x'_4 exchange between a hole-hole $(\vec{B}, A_4), (\vec{C}, D_4)$.

Since the vector particle is assumed to be self-dual, or propagation of x_4 is same as that of x'_4 , the hole-particle interaction between (\vec{C}, D_4) and (\vec{A}, B_4) represented in Fig.26. The particle-hole interaction between (\vec{D}, C_4) and (\vec{B}, A_4) can be obtained by performing the time reversal.

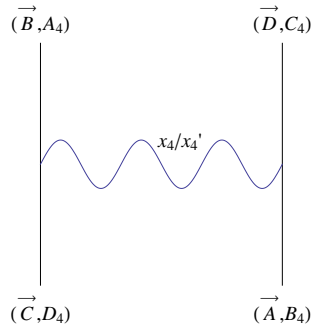


Figure 26: The vector x_4/x'_4 exchange between a hole-particle $(\vec{C}, D_4), (\vec{A}, B_4)$

In our analysis of MC circuit, we defined the voltage across the capacitor $x_1 = v_C(t)$, the current through the inductor $x_2 = i_L(t)$ and the internal state of the memristor $x_3 = z(t)$.

From the frequency ω of the single period oscillation observed in the widest window of the bifurcation diagram, we calculate $\omega/8$ and compare the ω/n of oscillation of periodicity equals to n . We observed a three periodic oscillation around $\omega = 0.375$, $\omega/3 = 0.125$, a four periodic oscillation around $\omega = 0.416$, $\omega/4 = 0.104$, and a five periodic oscillation around $\omega = 0.444$, $\omega/5 = 0.088$. ω divided by a number of periods n defined as ω/n is nearly linear function of $0.18 - 0.018n$, and n runs from 2 to 15.

In the case of $C = 1.2$, we observe windows of periodicity n from 2 to 9. The last window of periodicity 10 is broken at the high-frequency region. In the case of $C = 1.2$, we observed windows of $n = 2, \dots, 9$, which have the smooth n dependence of ω/n .

The 2nd order particle-particle interaction occurs through the Fig.27. The hole-hole interaction appears by performing the of (\vec{B}, \vec{C}) and (\vec{A}, \vec{D}) .

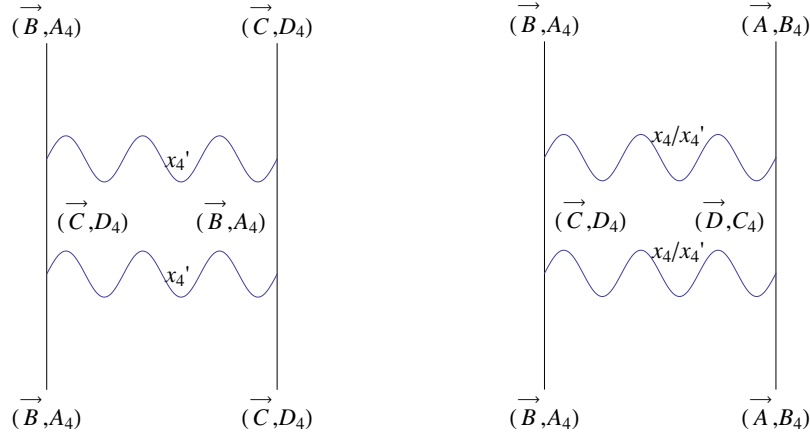


Figure 27: The double vector x_4 exchange between a hole-hole exchange between $(\vec{B}, A_4), (\vec{C}, D_4)$. Figure 28: The double vector x_4/x_4' exchange between hole-particle $(\vec{B}, A_4), (\vec{A}, B_4)$.

The particle-hole interaction is possible through double vector x_4/x_4' exchange is shown in Fig.28

6 Discussion

We studied the sinusoidally driven memristor circuit. We observed non-chaotic strange attractors and different from the case of driven Chua's circuit[20], we first observed period adding low as in LCR circuit[22]. In the case of $C = 1.2$, we observed a sequence of response frequency f_d stepwise increasing, and the winding number $W = f_s/f_d$ shows a sequence $W = \{\frac{1}{2}, \frac{2}{3}, \frac{3}{4}, \dots, \frac{8}{9}, \frac{1}{1}\}$ and Farey sum sequences $W = \{\frac{3}{5}, \frac{4}{7}, \dots, \frac{1}{2}\}$ and $\{\frac{5}{8}, \frac{7}{9}, \dots, \frac{2}{1}\}$. It is interesting that in the analysis of non-linear circuit of [21], the number of response P of the v_C , which corresponds to our f_d , was assigned as Level-2 devil's staircase sequence from step 2, and 8 steps $P = 2, 3, \dots, 9$ were considered as in our case of $C = 1.2$. The driving oscillation is $P = 1$, in their cases and their responses are not hidden oscillations.

In the case of $C = 1$, we find winding number's sequences $W = \{\frac{1}{2}, \frac{2}{3}, \frac{3}{4}, \dots, \frac{14}{15}, \frac{1}{1}\}$, but we do not find the Farey sum sequences observed in $C = 1.2$. It means that the way to chaos via the devil's staircase which is observed in the case of $C = 1.2$ is absent in the case of $C = 1$.

In the Level-2 devil's staircase sequence from step 3 to step 2 of [21], 7 steps $P = 3, 5, \dots, 15$ were considered.

When ω of $W = 1$ is divided by 8, it becomes close to ω of $W = \frac{6}{7}$ divided by 7. It suggests that the octonion that appears as a combination of two quaternions plays an important role in the circuit, since Dirac electrons are expressed by quaternions.

Oscillation in the voltage of two capacitances v_{C1}, v_{C2} and the current i_L of an inductor in nonlinear coupled circuits can be analyzed using the quaternion bases. In MC circuits, octonion plays an important role in the matching of period ω/f_d . Symmetry of electromagnetic field and that of probes must be studied together. We found nonchaotic strange attractors, or strange attractors whose Lyapunov exponent is negative, in the driven MC circuit.

The Poincaré map of the memristor current obtained by choosing the plane defined by the condition $Mod[\omega t, 2\pi] = 0$ shows a relatively complicated structure at a certain frequency region. When the amplitude of the external oscillation is small, the strange attractor remains nonchaotic, but when it is large, the strange attractor at a certain frequency region becomes

chaotic. The condition depends upon the capacity of the condenser C .

We considered vector particle interactions with electron particles and holes which are represented by octonions. It is not evident that the electrons and positrons could be represented by octonions, instead of a combination of quaternions, but it is worth studying the possibility of representing quarks and anti-quarks by octonions[31, 33, 34].

Acknowledgments

We thank Dr. Dos Santos for sending his thesis, which contains valuable information on the chaos via devil's staircase, and giving us helpful comments. Thanks are also due to Dr. F. Nakamura of Wolfram Research for a support in programming using Mathematica 9.

References

- [1] Hayes,S., Grebogi,C. and Ott,E.[1993], Communicating with Chaos, Rev. Mod. Phys. **70**, 2031-2034.
- [2] Eckman,J.-P. and Ruelle,D.[1985], Ergodic theory of chaos and strange attractors, Rev. Mod. Phys. **57**, 617.
- [3] Grassberger,P. and Procaccia, I.[1983], Measuring the Strangeness of Strange Attractors, Physica**9D**189-208.
- [4] Grebogi,C., Ott,E., Pelikan,S. and Yorke,J.A.[1984], Strange Attractors that are not Chaotic, Physica **13D**, 261.
- [5] Ding,M., Grebogi,C. and Ott, E.[1989], Dimension of Strange Non-chaotic Attractors, Phys. Lett. A**137**,167.
- [6] Heagy,J.F. and Hammel, S.M.[1994], The birth of strange nonchaotic attractors, Physica **D70** 140-153.
- [7] Keller,G.[1996], A note on strange nonchaotic attractors, Fundamenta Mathematicae **151**, 139.
- [8] Grendinning,P.[2002], Global attractors of pinched skew products, Dynamical Systems **17**, 287.
- [9] Alsedà,L. and Misiurewicz, M.[2008], Attractors for unimodal quasiperiodically forced maps, Journal of Difference Equations and Applications, **14** 1175.
- [10] Gröger,M. and Jäger,T.[2013], Dimension of Attractors in Pinched Skew Products, arXiv:1111.6574 v2[math.DS].
- [11] Chua,L.O.[1971], Memristor-The Missing Circuit Element, IEEE Transactions on Circuit Theory, **CT-18**, 507.
- [12] Chua,L.O. and Kang,S.M.[1976], Memristive Devices and Systems, Proceedings of the IEEE, **64**, 209.
- [13] Muthuswamy,B. and Chua, L.O.[2010], Simplest Chaotic Circuit, International Journal of Bifurcation and Chaos, **20**, 1567.

- [14] Ginoux,J.-M. and Letellier, Ch.[2009], Flow curvature manifolds for shaping chaotic attractors: I. Rössler-like systems, *J. Phys. A: Math. Theor.* **42**, 285101-17.
- [15] Gilmore, R., Ginoux,J-M., Jones,T., Letellier,C. and Freitas,U.S.[2010], Connecting curves for dynamical systems, *J. Phys. A: Mathe Theor.* **43**, 255101-13.
- [16] Ginoux,J.M., Letellier,Ch. and Chua,L.O.[2010], Topological Analysis of Chaotic Solution of Three-Element Memristive Circuit, *International Journal of Bifurcation and Chaos* **20**,3819-3827.
- [17] Chua,L.O.[2011], Resistance switching memories are memristors, *Appl. Phys.* **A 102**, 765-783.
- [18] Chua,L.O., Komuro,M. and Matsumoto,T.[1986], The Double Scroll Family, *IEEE Transactions on Circ.Syst*, **CAS33**,1073.
- [19] Saito,T. and Nakano,H.[2003], Chaotic Circuits Based on Dependent Switched Capacitors, CP676 *Experimental Chaos*, AIP Proceedings, 3-13.
- [20] Pivka,L., Zheleznyak,A.L. and Chua,L.O.[1994], Arnold's Tongues, Devil's Staircase and Self-similarity in the Driven Chua's Circuit, *International Journal of Bifurcation and Chaos* **20**,1743-1753.
- [21] Chua,L.O., Yao,Y. and Yang,Q.[1986], Devil's Staircase Route to Chaos in a Non-Linear Circuit, *Circuit Theory and Applications*, **14**, 315-329.
- [22] Manimehan,I., Thamilmaran,K., Chidambaram,G. and Philominathan, P. [2005], Transition From Torus To Chaos In A Piecewise-linear Forced Parallel LCR Circuit, *National Conference on Nonlinear Systems & Dynamics*, 1-4.
- [23] Zhu,Z. and Liu,Z.[1997], Strange Nonchaotic Attractors of Chua's Circuit with Quasiperiodic Excitation, *International Journal of Bifurcation and Chaos*, **7**, 227-238.
- [24] Baptista,M.S. and Cardas,I.L.[1998] , Phase-Locking and Bifurcations of the Sinusoidally-Driven Double Scroll Circuit, *Nonlinear Dinamics* **17**, 119-139.

- [25] Thamilmaran,K. and Lakshmanan,M. [2002], Classification of Bifurcations and Routes to Chaos in a Variant of Murali-Lakshmanan-Chua Circuit, International Journal of Bifurcation and Chaos **12**, 783-813.
- [26] Leonov,G.A., Vagaitsev,V.I. and Kuznetsov,N.V.[2010], Algorithm for Localizing Chua Attractors Based on the Harmonic Linearization Method, ISSN 1064-5624, Doklady Mathematics 2010, **82**, 663-666.
- [27] Leonov,G.A. and Kuznetsov,N.V.[2013] Hidden Attractors in Dynamical Systems, From Hidden Oscillators in Hilbert-Kolmogorov, Aizerman, and Kalman Problems to Hidden Chaotic Attractor in Chua Circuits, International Journal of Bifurcation and Chaos **23**, 1330002-1-69.
- [28] Furui,S. and Niiya,S.[2007], Shilnikov chaos control using homoclinic orbits and the Newhouse region, Chaos, Solitons and Fractals, **34**, 966-988.
- [29] Pikovsky,A. and Feudel,U.[1997], Comment on "Strange nonchaotic attractors in autonomous and periodically driven system", Phys. Rev. E, **56**,7320-7321.
- [30] Cartan,É.[1966] "The Theory of Spinors", Dover Pub.
- [31] Furui,S.[2012] Fermion Flavors in Quaternion Basis and Infrared QCD, Few-Body Syst **52**, 171-187.
- [32] Dos Santos,S.[1998] Étude non linéaire et arithmétique de la synchronisation des systèmes: application aux fluctuations de basse fréquence des oscillateurs ultra-stables, *Thèse Grade de Docteur de l'Université de Franche-Comté*
- [33] Furui,S.[2013a] Chaos in Electronic Circuits and Studies of Bifurcation Mechanisms, Proceedings of International Conference of Numerical Analysis and Applied Mathematics 2013(ICNAAM2013), Rhodes, AIP proceedings 1558, p.2233-2236.
- [34] Furui,S.[2013b] Clifford Algebra and Physical and Engineering Sciences, Proceedings of International Conference of Numerical Analysis and Applied Mathematics 2013(ICNAAM2013), Rhodes, AIP proceedings 1558, p.521-524.